

## Chapter 2 Experimental

### 2.1 Materials

#### 2.1.1 Epoxy Resins

A solventborne epoxy impregnating system was prepared from Shell Epon<sup>®</sup> 828, a DGEBA liquid epoxy resin having a molecular weight per epoxide group (WPE) of 190, with a DICY curing agent (Air Products Amicure<sup>®</sup> CG-1200) and an accelerator, 2-methylimidazole (2-MI). These solid powder curing agents were dissolved in warm N, N-dimethyl formamide (DMF) in DICY concentrations ranging from 1 phr to 6 phr and 0.3 phr 2-MI, and stirred into the 828 resin, maintaining the agitation to room temperature. A corresponding waterborne epoxy system was prepared from Shell Epi-Rez<sup>®</sup> 3510-W-60, an aqueous dispersion of DEGBA resin (WPE = 195). The same DICY and 2-MI curing agents described above were dissolved in warm deionized (DI) water and stirred into the 3510 resin; curing agent concentrations, varying from 1 to 6 phr, were based on the weight of the epoxy fraction of the emulsions. Additional Triton X-100 surfactant, in experiments that called for it, was dissolved in the warm DI water along with the curing agents prior to mixing with the latex emulsion. Weight percent additions of surfactant were also computed on an epoxy mass fraction basis.

#### 2.1.2 Epoxy/Glass Laminates

The glass reinforcement used in this study was a plain weave 2116 E-glass cloth having a density of 109 g/m<sup>2</sup> (3.22 oz/ yd<sup>2</sup>) and a thickness of 0.096 mm (0.0038) inches, sized with aminopropyltrimethoxy silane, supplied by Clark-Schwabel. Squares of cloth measuring 14 cm x 14 cm (5.5 in x 5.5 in) were cut from the bolt and stored in a drying oven at approximately 90°C for at least 12 hours prior to resin impregnation. The cloth squares were dip-coated through a bath of room temperature epoxy resin/curing agent solutions mixed as described above. The impregnated cloth (prepreg) was then placed on a 2-mil (.05 mm) teflon release film supported by a rigid glass or polypropylene plate. This wet prepreg glass cloth was allowed to dry in an environmentally controlled chamber described in Section 2.3.5. Once dry and fully coalesced, usually overnight, the tacky prepreg was covered by a second layer of teflon release film and stored in a freezer to minimize the advancement of cure. Sheets of uncured prepreg were cured to an intermediate level (known as B-stage) by placement (still layered between teflon release film) between 15.2 cm x 15.2 cm (6 in x 6 in) aluminum plates and hot-pressing under contact pressure at 150°C for 2.5 to 3 minutes. This B-staged ply was then cut into smaller squares for stacking and laminating.

Both copper foil-clad and unclad laminates were produced for various experiments. The B-staged prepreg plies were stacked and placed between mirror finished steel laminating plates in a Carver laminating press, using coarse paper as the bleeder cloth and 2 mil teflon as the release film. A schematic of the laminating

technique is shown in Figure 2.1. Eight ply laminates of epoxy/glass prepreg, were cured at 180°C for 1 hour at a pressure of about 1400 kPa (200 psi). PCB peel specimens were fabricated by layering 1-ounce (0.036 mm thick) copper foil (Gould Electronics, Inc.) on both surfaces of the glass/epoxy laminates and pressing under the same conditions.

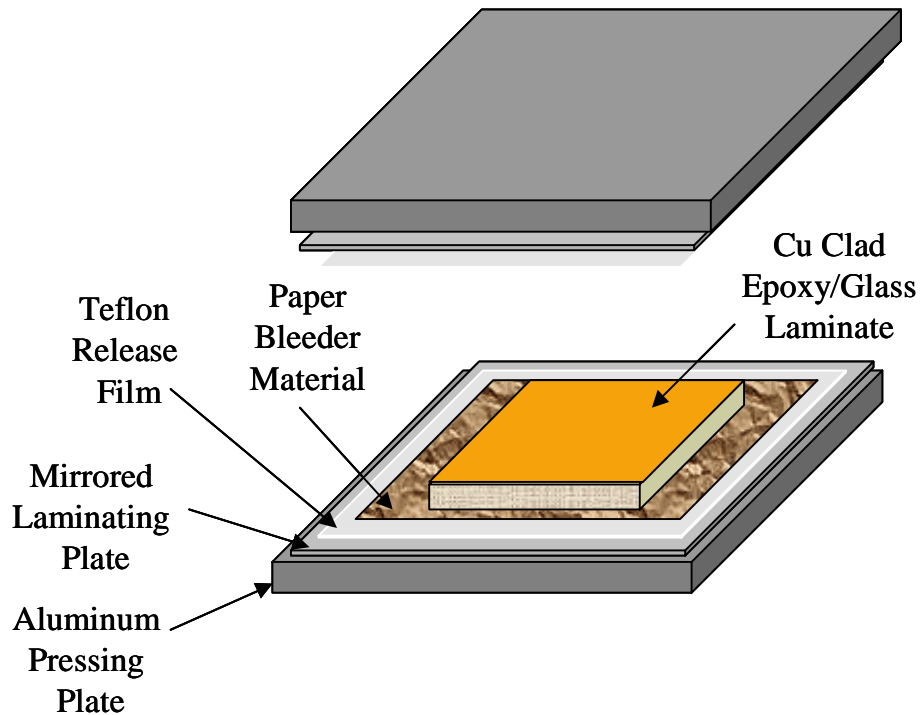


**Figure 2.1: Copper foil clad laminate fabrication schematic**

### **2.1.3 Copper Surface Preparation**

In addition to the factory supplied “brass” treated copper foil, a brown oxide copper surface treatment was used in PCB fabrication. The brown oxide was formed using heated sodium chlorite treatment, described by the following process steps:<sup>1</sup>

- 1) Prepare a sodium persulfate etching solution (20g  $\text{Na}_2\text{S}_2\text{O}_8$  /L DI  $\text{H}_2\text{O}$ ) and a sodium chlorite oxidizing solution (160g  $\text{NaClO}_2$  + 10 g  $\text{NaOH}$  /L DI  $\text{H}_2\text{O}$ )
- 2) Abrade the untreated surface of 1-oz copper foil with 400 grit SiC sandpaper
- 3) Immerse the abraded foil in the room temperature sodium persulfate etching solution for 4 minutes, remove, rinse by flooding with DI water, and blow-dry with  $\text{N}_2$  gas
- 4) Immerse the etched foil in the sodium chlorite oxidizing bath, controlled at 86°C, for four minutes, remove, rinse by flooding with DI water, and blow-dry with  $\text{N}_2$
- 5) Place the oxidized foil in a 60°C drying oven overnight

A temperature controlled covered bath, shown schematically in Figure 2.2, was used in the oxidizing step (4). Temperatures were maintained within an estimated  $\pm 3^\circ\text{C}$ . The cover maintained the proper concentration of the oxidizing solution by preventing evaporation.

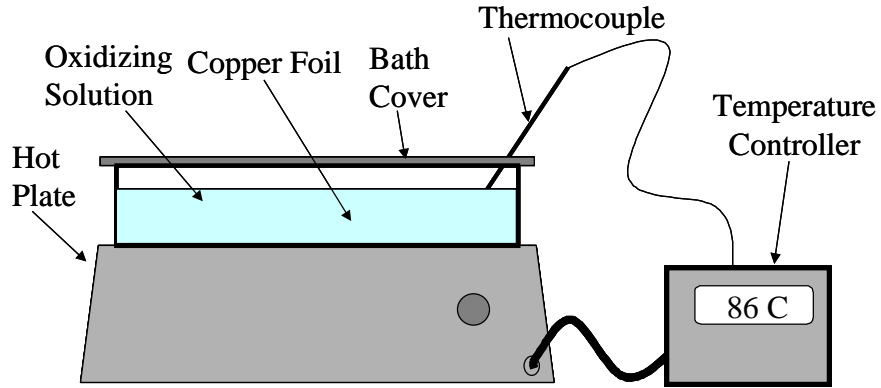


Figure 2.2: Schematic of the temperature-controlled copper oxidizing bath used in foil treatment

## 2.2 Sample Preparation

### 2.2.1 Peel Specimens

PCB laminates having nominal dimensions of 7 cm x 7 cm (2.75 in. x 2.75 in.), copper foil-clad on both surfaces, were fabricated using the process described in Section 2.1.2. A schematic of the typical peel coupon geometry is shown in Figure 2.3. Copper clad laminates were edge-trimmed and lightly sanded with 400 grit SiC paper, prior to masking, to remove any epoxy from the surface that might act as a barrier to the etching solution. A pattern of peel strips nominally 3.2 mm in width was formed on both sides of the clad laminate by masking with an adhesively backed vinyl film mask (Roland Digital Group), and etching by immersion in a commercial ferric chloride solution (Radio Shack) under moderate agitation at room temperature for 15 minutes. The laminate was thoroughly rinsed in DI water upon removal from the etching solution, the vinyl mask was removed, and the etched laminate was placed in a drying oven overnight at  $90^\circ\text{C}$  prior to testing.

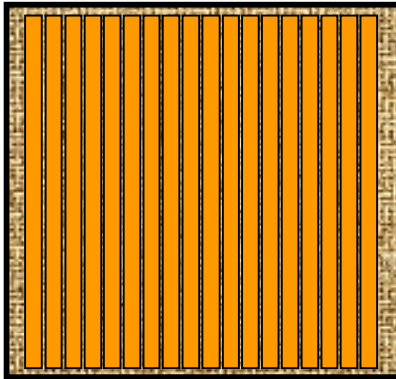


Figure 2.3: Schematic of a typical peel coupon used for PCB adhesion studies.

## **2.2.2 Dielectric Measurement Specimens**

### **2.2.2.1 Microwave Frequency Analysis Samples**

Neat epoxy resin and laminate materials were prepared as described in Sections 2.1.1. Neat resin specimens were cast in molds of dimensions 38.0 x 3.0 x 1.5 mm and cured for 1 hour at 180°C. Eight-ply, cured epoxy impregnated laminates were fabricated and cut to dimensions of 2 x 0.5 x 50 mm. To remove any surfactant that might be available for moisture sorption, several neat waterborne epoxy specimens were exposed to boiling water in a Soxhlet extraction column for 72 hours and dried. These samples were designated “extracted” while another set of waterborne samples, which remained in the as-made condition, were designated “unextracted”.

These neat resin and resin impregnated composite specimens were exposed to different moisture environments to determine how water absorption affects the material’s dielectric properties. The extracted samples were tested in parallel with as-made unextracted samples. Dry samples were conditioned in an environmental chamber at elevated humidities and temperatures to gradually increase their moisture content. The dielectric properties of the samples were measured after reaching mass equilibrium in each environment, as determined by repeated weighing until no further mass gain (within  $\pm 0.0003$  g) was observed. Samples were then saturated by immersion in boiling water, with their dielectric properties periodically measured at room temperature using the cavity perturbation technique at 9.4 GHz as described in Section 2.3.4.1.

### **2.2.2.2 Dielectric Analysis (DEA) Samples**

Neat resin and PCB laminate materials were produced from solventborne and latex epoxy resins as described in Section 2.1. The nominal thickness of the neat resin samples was 0.5 mm, while the laminates were an eight-ply construction having a thickness of 0.7 mm. Samples of both materials were cut into planar samples with dimensions of 25.4 mm x 25.4 mm (1 in. x 1 in.). Samples were oven dried at 80°C overnight then stored in a desiccated container prior to testing. Immediately prior to dielectric testing representative samples were selected from each material batch, weighed, thoroughly dried at 110°C under vacuum, and reweighed. A maximum weight loss of 0.1 % was observed; it is therefore believed that moisture effects were minimal during dielectric testing.

## **2.3 Measurement and Analysis**

### **2.3.1 Peel Testing**

#### **2.3.1.1 The 90° Peel Test**

Peel testing was the primary method for determining copper/epoxy adhesion. The strain energy release rate of the peel process has been approximated:<sup>2,3</sup>

$$\text{Equation 2.1} \quad G = \frac{P}{w}(1 - \cos \theta)$$

where  $G$  is the strain energy release rate,  $P$  is the applied peel force,  $w$  is the width of the peel specimen, and  $\theta$  is the peel angle.

Equation 2.1 assumes very small axial strains in the flexible adherend being peeled; this assumption is valid in the current study given the relatively low loads involved with the peel of copper/epoxy bonds.

Significant plastic deformation does occur, however, in the bending of a thin copper foil adherend undergoing  $90^\circ$  peel. A conservative estimate of the peel force associated with the plastic deformation in a  $90^\circ$  peel geometry is given by Gent and Hamed:<sup>4</sup>

$$\text{Equation 2.2} \quad P_{90} = \frac{t^2 \sigma_y}{4R}$$

where  $P_{90}$  is the maximum force per unit strip width contribution from plastic adherend deformation in bending,  $t$  is the adherend thickness,  $R$  is the radius of curvature of the neutral axis of the peel strip, and  $\sigma_y$  is the adherend material's yield stress. Equation 2.2 requires an estimate of the radius of curvature of the bending foil strip under peel loading conditions. A representative copper peel strip has been examined by optical microscopy as shown in Figure 2.4. This strip has been imaged while under  $90^\circ$  loading sufficient to propagate fracture and therefore meets the conditions for employing the model of Gent and Hamed. A radius of curvature was estimated from the image in Figure 2.4 to be 0.3 mm. Tensile tests were conducted on 7 samples of the same copper foil used in laminating the PCB peel samples resulting in an average yield strength  $\sigma_y$  of  $397 \pm 8$  MPa. The thickness,  $t$ , of the peeled strip was 0.02 mm. When these data are substituted into Equation 2.2, a maximum  $90^\circ$  peel force  $P_{90}$  is computed to be approximately 130 N/m. Typical copper-epoxy as-made peel strengths measured in this study were 1200 to 1500 N/m, hence the plastic deformation in the adherend contributes a *maximum* of approximately 10% of the overall peel strength. It must be recalled that this plastic deformation contribution will be encountered in all of the results that have similar strengths; therefore comparisons of relative strengths between different material systems are still valid. For this reason the plastic deformation contribution to the overall peel strength will be ignored in the data presented in this study.

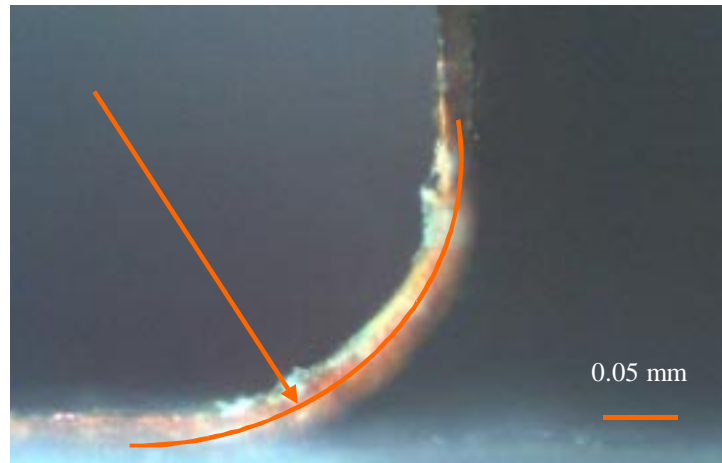


**Figure 2.4: Photomicrograph of 1 oz. copper foil undergoing 90° peel from a glass-epoxy laminate. The radius of curvature of the neutral axis is highlighted.**

The peel test method used in this study is similar to one developed for copper clad flexible films as detailed in ASTM D 2861-87.<sup>5</sup> This method is essentially a quasi-constant 90° peel test where strips of copper are pulled from the surface of the glass/epoxy laminate to which they are adhered. The copper strip is gripped by a clamp which is connected to the cross-head of a tensile frame by a light, flexible chain. A slotted metal frame fixtures the laminate on the base of the tensile frame as shown in Figure 2.5. The slot through which the copper strip passes is designed to be slightly wider than the peel strip, thereby allowing only local, small-scale flexure of the substrate laminate. This constraint of the substrate's flexure serves to minimize the effects of variability in laminate stiffness due to plasticization or degradation. Peel tests were conducted using a TA-XT2i Texture Analyzer tensile frame.

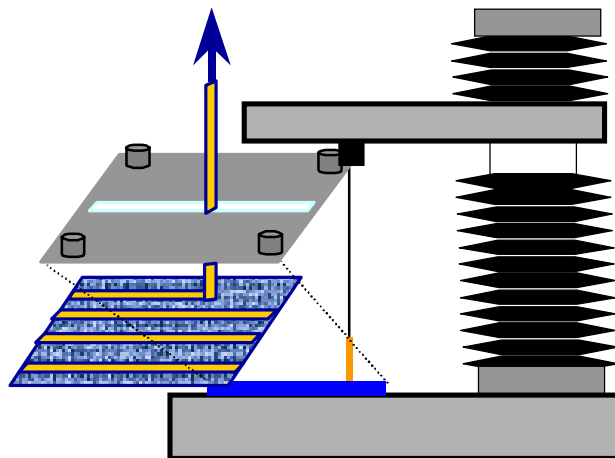


**Figure 2.5: The TA-XT2i Texture Analyzer tensile frame with a 90° PCB peel test fixture**

An estimate of the error in the application of Equation 2.1, associated with this test geometry's deviation from pure 90° peel, has been conducted by using the chain and clamp length of 112 mm and peeling a standard specimen. The maximum chain and peeled specimen length were measured, as was the horizontal travel from the vertical axis of force application. These data were used to compute a maximum angular deviation from pure 90° peel of about 6°, which contributes approximately a 12% error. Note that this represents only the maximum error encountered at the extremes of the test; the majority of the test, which falls much closer to the 90° assumption, is averaged with these extremes to yield a much smaller error related to peel angle deviation. Strength results from four peel strips, for any given test condition, were averaged and standard deviations computed; these data are presented in the plots of Chapter 4.

### 2.3.1.2 Viscoelastic Peel Study

The as-made condition of the copper-epoxy interface was evaluated by conducting 90° peel tests at three different rates, 0.1, 1, and 10 mm/s, and four temperatures in a range from 50°C to approximately 140°C. Peel data obtained under these conditions were used to gain an understanding of the adhesive response of the copper/laminate system by applying the time-temperature superposition techniques to be described in Chapter 4. PCB specimens were fabricated using solventborne epoxy and waterborne latex epoxy resin containing 5, 10 and 15 wt % concentrations of surfactant. A heated enclosure, shown schematically in Figure 2.6, was constructed to conduct elevated temperature peels. The temperature of the peel specimen was sensed by a thermocouple placed between the lower surface of the specimen and the insulated enclosure floor. A digital temperature controller, which switched power to heating tapes adhered to the enclosure's walls, monitored this thermocouple's signal. An independent digital thermometer monitored the temperature of the upper surface of the specimens. Peel specimens equilibrated for 5 to 10 minutes prior to testing based upon the equalization of the upper- and lower surface temperatures.

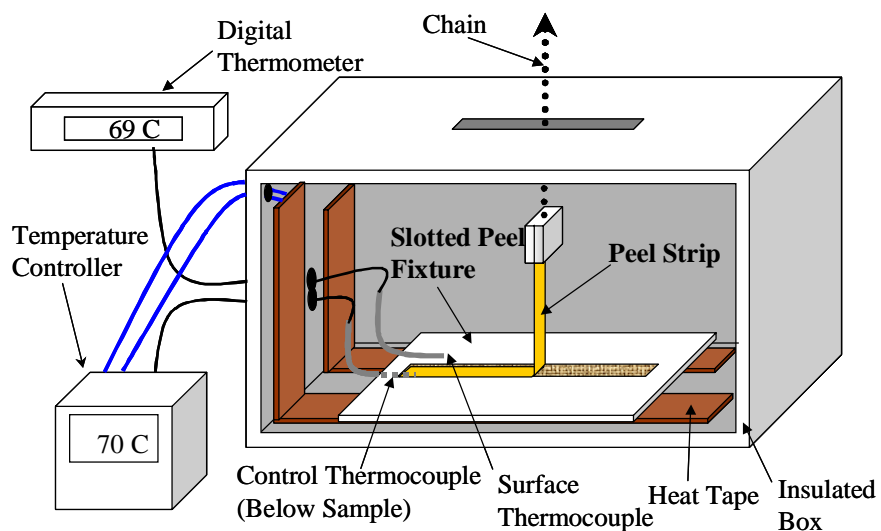


Figure 2.6: Temperature controlled peel test enclosure schematic

### 2.3.1.3 Elevated Temperature Peel Durability Study

The thermal aging component of this study is motivated by the need to evaluate the waterborne latex epoxy system's ability to survive simulated processing conditions in PCB manufacture while delivering adhesive and structural performance comparable to that of standard solventborne resins. In the case of DICY cured DGEBA impregnated laminates, common processing cycles consist of 1 to 2 hours heating at 180°C. In multilayer circuit assemblies this cure cycle may be repeated many times, thereby increasing the elevated temperature durability requirements placed upon the resin system.

Copper clad laminates were fabricated using 1 oz (0.0036 cm thick) zinc chromate ("brass") and brown oxide treated foils for adhesion testing. The support laminates were impregnated with solvent- and waterborne epoxy resins, the latter containing varied levels of added surfactant to study its effect on adhesive stability. Peel test coupons of the type shown in Figure 2.3 were etched in a pattern of 18 peel strips per surface, and dried. Copper strips from each test coupon were peeled in the as-made condition and the strengths recorded. The coupon was then aged at an elevated temperature for a predetermined length of time, cooled, and peeled at room temperature. Samples were tested at a peel rate of 1mm/s. Both the peel strip and a section of PCB coupon that formed the substrate interface were cut from the coupon and archived for surface analysis as representative of its thermal aging condition. This age-and-peel process was repeated using four foil strips, with two strips selected from each side of the PCB specimen, for each aging condition. Aging temperatures were in a range of 160°C to 220°C. Samples were aged by placing them between 1.27 cm (0.5 in) thick aluminum laminating plates lined with 2 mil teflon film, inserting them into a preheated platen press, and applying contact pressure. After aging for a prescribed time, the samples were removed from the hot platens and immediately placed between water-cooled platens. Cooling from the aging temperature to 50°C occurred in approximately 5 minutes, for a cooling rate of 25 to 30°C/minute.

SEM was used to examine the morphology of the failure surface, while XPS and IR analyses were employed to provide an understanding of the chemistry of the failed surface. Possible failure mechanisms may include fracture in the copper oxide layer, debonding in weak surfactant- or DICY-rich boundary layers at the interface, and degradation of the epoxy network due to catalytic chain scission by the copper oxides.

### 2.3.2 Dynamic Mechanical Analysis

Shifts in the glass transition temperature and modulus of thermally aged neat resins and impregnated laminates were measured using DMA. The presence of miscible surfactant will depress the  $T_g$  of an epoxy network, while surfactant segregation out of the epoxy bulk to the foil or fiber interfaces will increase the overall  $T_g$  of the system.  $T_g$  will also increase due to more complete cross-linking reactions occurring at



elevated temperatures. Conversely, large-scale thermally induced chain scission would decrease the cross-link density, lowering both the  $T_g$  and the modulus of the material.

The instrument used in this study was a Perkin-Elmer DMA 7 controlled by Pyris data acquisition software. Epoxy-glass laminates and neat resins were measured in the three-point bending mode shown schematically in Figure 2.7. Support span widths of 5mm and 10mm were used for neat resin samples and laminates, respectively. Measurements were conducted at a frequency of 1 Hz, in the amplitude control mode, with amplitudes set at 10  $\mu\text{m}$ . All experiments were conducted in an argon atmosphere to prevent oxidative degradation of the samples. Two temperature profiles were employed: a hold and heat program for simple  $T_g$  measurements and a cycled hold-heat-hold-cool program for a postcure study described in Section 4.2.3. All heating ramp rates were 2.5°C/minute. A 10°C/minute cooling rate was employed in the postcure program. Samples were equilibrated at the initial temperature for a minimum of three minutes prior to starting the experiment. Cross-sectional dimensions for neat resin and laminate samples were nominally 4.0 mm x 0.7 mm and 3.0 mm x 0.4 mm, respectively. The DMA system was calibrated using a two-point method with indium and zinc standards, and was periodically checked with indium.

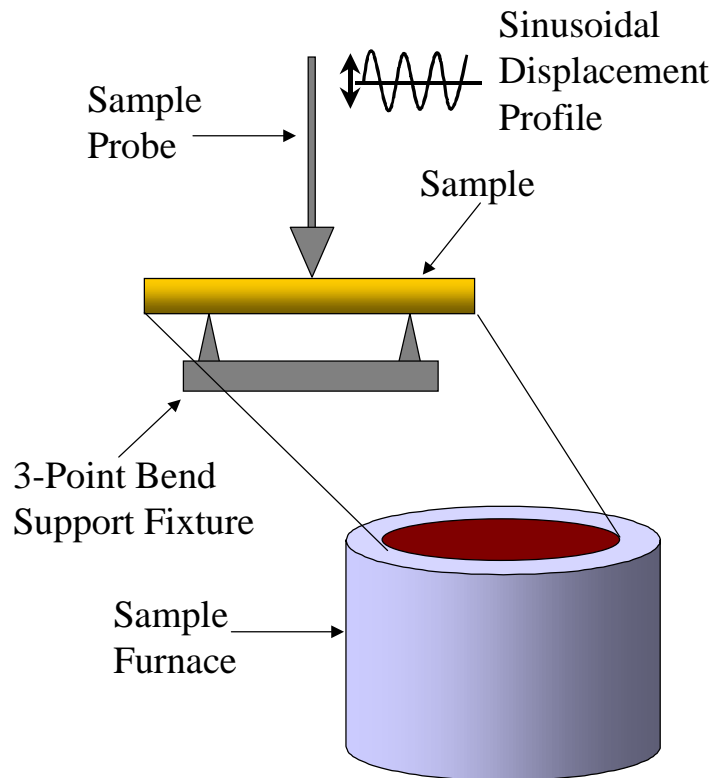


**Figure 2.7: Schematic of the three point bend configuration used in DMA testing**

### 2.3.3 Thermogravimetric Analysis

Thermogravimetric Analysis (TGA) involves the measurement of weight change in a material as it is heated. This method is commonly used in polymer thermal stability studies to find volatilization temperatures and to determine the mass fraction of inorganic fillers.<sup>6</sup> A Perkin-Elmer vertical TGA 7 was used in this study to determine the fiber weight fraction of peeled PCB laminates, and to determine any differences in the thermal degradation behavior in these laminates due to the presence of residual surfactant. Samples weighing approximately 15 mg were cut from dry laminates and placed in a platinum sample pan suspended from the TGA's microbalance. The furnace tube was then raised and the experiment started. Bottled air was used as the purge gas for the sample chamber, while the balance compartment was purged with nitrogen. Samples were heated from 50°C to 850°C at 5°C/minute. Mass loss data were used to generate the weight fraction versus temperature curves shown in Figure 2.8. The large weight loss observed around 400°C corresponds to scission of the main chains in the epoxy network.<sup>7</sup> Final steady-state weight fractions represent the fiber mass fractions of the composite. Upon completion of the TGA experiment, the samples were reduced to glass fibers burned white and completely clean. First derivative curves of weight fraction as a function of temperature ( $dW/dT$ ) are shown, in Figure 2.9, to be essentially identical. Hong and Wang<sup>7</sup> found that shifts in  $dW/dT$  peaks, as measured by TGA, were proportional to the activation energies of the degradation processes in epoxy materials. The similarity of the  $dW/dT$  curves shown in Figure 2.9 suggests that the presence of increasing surfactant concentrations does not appreciably decrease the thermal stability of the epoxy matrix.

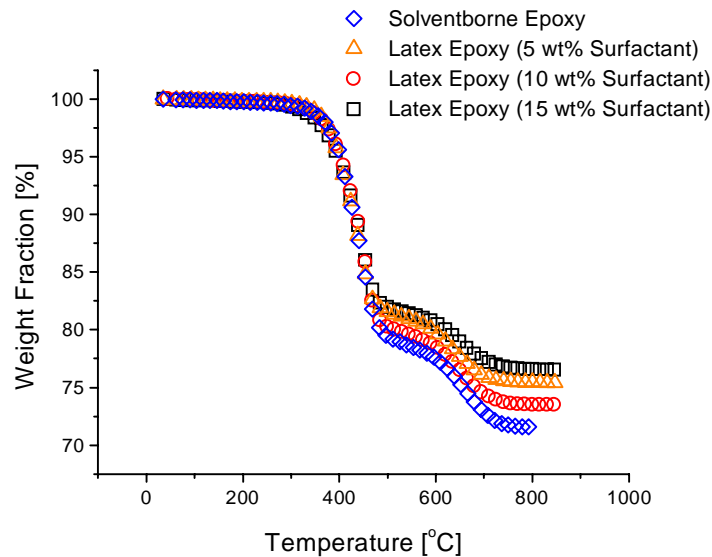


**Figure 2.8: Laminate weight fraction curves during thermal decomposition as measured by TGA**

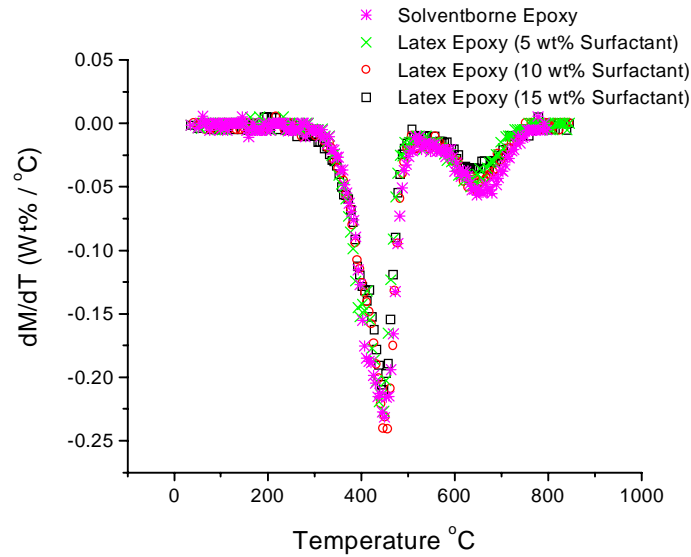


**Figure 2.9: First derivative curve of weight fraction versus temperature for laminate materials**

### 2.3.4 Dielectric Measurement

#### 2.3.4.1 Microwave Frequency Measurement

Measurement of the microwave frequency dielectric properties was carried out using the cavity perturbation technique which is based on the measurement of the shift in the state of a resonant cavity upon introduction of a small dielectric sample into the geometric center of the cavity as shown in Figure 2.10.<sup>8</sup> This technique assumes little change in the electric field structure due to the insertion of the small sample; samples having large dielectric constants can significantly alter the electric field structure, leading to increased measurement uncertainty. Shifts in the cavity's resonant frequency upon insertion of a dielectric sample are proportional to the dielectric constant  $\epsilon'$ , representing the real part of the complex permittivity. These shifts correspond to changes in the cavity's energy state in the form of stored electric field as

$$\text{Equation 2.3} \quad \epsilon' = \frac{V_c (f_{r0} - f_{r\epsilon})}{2V_\epsilon f_{r0}} + 1$$

where  $V_c$  and  $V_\epsilon$  are the volume of the resonant cavity and the dielectric sample, respectively, and  $f_{r0}$  and  $f_{r\epsilon}$  are the resonant frequencies of the empty cavity and sample-loaded cavity, respectively. A shift in the cavity's ability to maintain its resonant nature, known as its quality factor  $Q$ , upon the introduction of a sample is related to the dielectric loss of the material  $\epsilon''$ , the imaginary part of the complex permittivity as

$$\text{Equation 2.4} \quad \epsilon'' = \frac{V_c}{4V_\epsilon} (1/Q_\epsilon - 1/Q_0)$$

where  $Q_0$  and  $Q_\epsilon$  represent the quality factor of the empty and sample loaded cavities, respectively. A decreased quality factor upon sample insertion represents energy dissipation through the material's interaction with the electric field.<sup>9</sup> The quality factor can be determined as

$$\text{Equation 2.5} \quad Q = \frac{f_0}{\Delta f}$$

where  $f_0$  is the resonant frequency and  $\Delta f$  is the width of the resonance peak 3dB from the maximum. The ratio of a material's dielectric loss to its electric field energy storage capacity is defined as its  $\tan \delta$ , where  $\tan \delta = \epsilon''/\epsilon'$ .

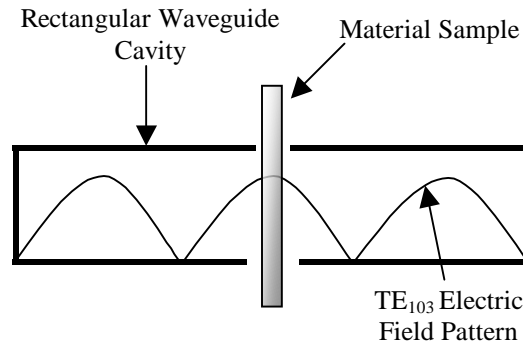


**Figure 2.10: Schematic of the cavity perturbation geometry using a resonant TE<sub>103</sub> rectangular waveguide cavity**

The dielectric experimental system was composed of a Hewlett Packard 8510B Vector Network Analyzer (VNA), an HP 8515A S-Parameter Test Set, an HP 8340A Synthesized Sweeper, a resonant TE<sub>103</sub> rectangular X-band waveguide cavity (Figure 2.10), and a HP 9000 Series 300 Computer as shown in Figure 2.11.<sup>10</sup> The 8510B VNA measured the complex impedance of the cavity by sweeping through resonance as a function of frequency in a reflection mode; the cavity's resonant frequency and Q factor were subsequently determined from this impedance circle using an 11 point interpolation method.<sup>11</sup>

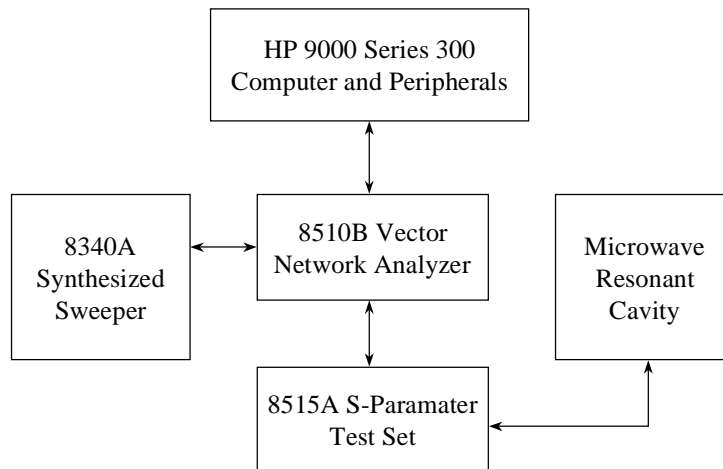


**Figure 2.11: Schematic of the microwave frequency dielectric measurement system**

#### **2.3.4.2 Dielectric Thermal Analysis**

The dielectric measurements in this part of the study were performed using the TA Instruments Dielectric Analyzer (DEA) 2970. This instrument imposes an oscillating voltage on a material sample through a pair of electrodes and measures the amplitude and phase of the current response using a microprocessor controlled detector. A parallel plate electrode configuration was used for the measurement of neat resin and laminate samples. The liquid surfactant was characterized using a planar sensor consisting of an interdigitated array of excitation and response electrodes. An exploded view schematic of the DEA 2970 parallel sensor and furnace assembly is shown in Figure 2.12. Both electrode types consisted of ceramic support plates patterned with gold-film electrodes. The sample temperature was monitored by a platinum resistance thermistor patterned on the interdigitated plate and on the excitation electrode of the parallel plate pair. Good electrode/sample contact was maintained at a controlled force level applied through a positioning ram supporting the upper electrode. A linear variable displacement transducer (LVDT) precisely tracked the sample thickness changes during temperature excursions for more accurate computation of the dielectric constants. The electrode and furnace assembly were constantly purged with dry nitrogen for the duration of each measurement.

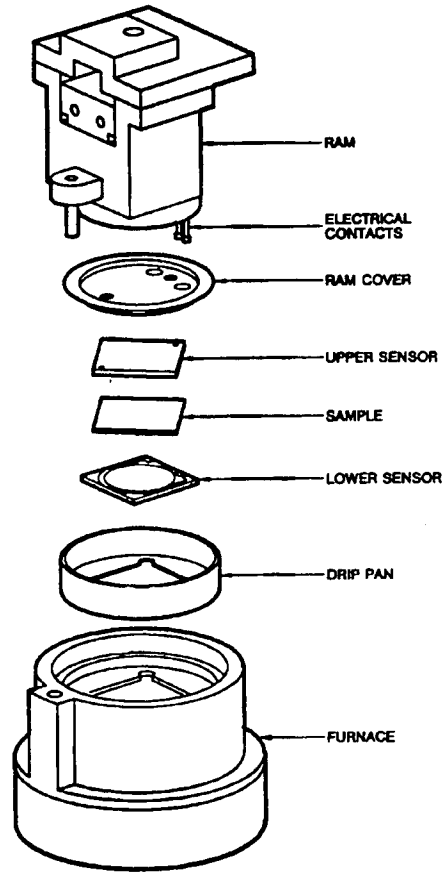


**Figure 2.12: Exploded view schematic of the DEA 2970 parallel plate electrode and furnace assembly<sup>12</sup>**

The parallel plate technique forms the cornerstone of measurement techniques for characterizing the dielectric properties of insulating solids, and to some degree liquids, in the DC to MHz frequency range. It is essentially based on the design of fundamental parallel plate capacitors where the relative dielectric constants are calculated:<sup>12</sup>

$$\text{Equation 2.6} \quad \epsilon' = \frac{Cd}{A}$$

$$\text{Equation 2.7} \quad \epsilon'' = \frac{d}{2\pi f R A}$$

where  $C$  is the measured capacitance [Farads],  $d$  is the plate separation distance [m],  $R$  is the measured resistance [Ohms],  $f$  is the frequency [Hz], and  $A$  is the plate area [m<sup>2</sup>]. The fundamental quantities of capacitance and resistance are determined by finding the phase shift angle  $\theta$  in measured current response,  $I_{\text{meas}}$  [Amperes], relative to an applied sinusoidal voltage,  $V_{\text{appl}}$ , [Volts] across the sample-loaded parallel plate capacitor as shown in Figure 2.13. This measured current phasor can be decomposed into pure

capacitive and pure resistive components as illustrated in Figure 2.14. Mathematically the capacitance and resistance are represented by

$$\text{Equation 2.8} \quad C = \frac{I_{meas} \sin \theta}{V_{appl} 2\pi f}$$

$$\text{Equation 2.9} \quad \frac{I}{R} = \frac{I_{meas} \cos \theta}{V_{appl}}$$

Capacitance measurements made with the electrode plates empty (or air filled) can be used to calibrate fixed system capacitances when measuring with the material in place. The DEA 2970 employs an automatic multipoint calibration procedure where the capacitance of empty electrodes is measured at various plate separation distances. The measurement resolution of the DEA 2970 at 1 kHz for  $\epsilon'$  is 0.01 and for  $\tan \delta$  is  $1 \times 10^{-4}$ , with a frequency capability range from 0.01 Hz to 100 kHz.

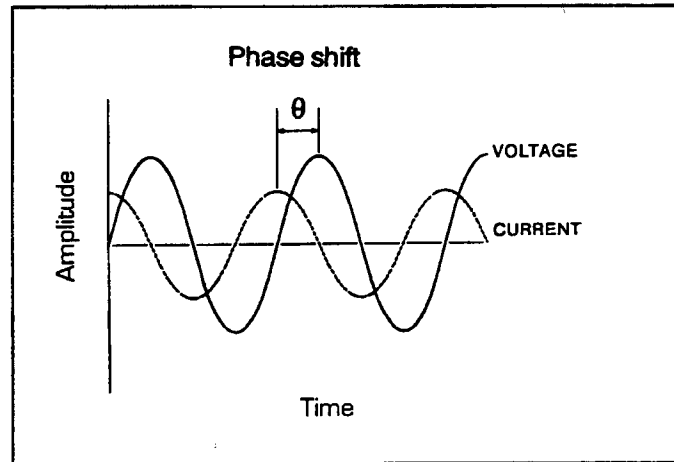
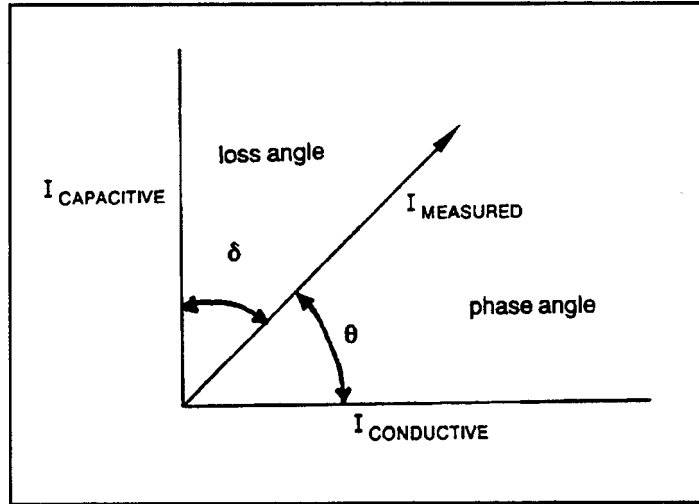
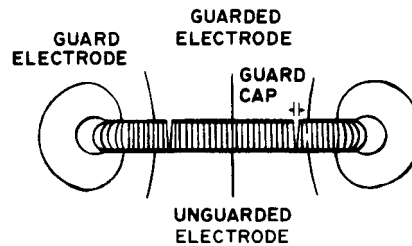


Figure 2.13: Phase shift in the current response to an applied sinusoidal voltage<sup>12</sup>



**Figure 2.14: Phasor representation of the measured current decomposed into conductive and capacitive components<sup>12</sup>**

Accounting for and minimizing fringing and stray capacitance is a key to the usefulness of this technique for precision measurements. Using electrodes with guard-rings, as shown in Figure 2.15, can minimize edge-fringing effects. These rings maintain a relatively uniform field pattern between the measurement electrodes, effectively moving the edge fringes well away from the actual measurement electrode. The parallel plate electrodes used in the DEA 2970 system include a guard ring on the response electrode and an unguarded excitation electrode similar to the configuration shown in Figure 2.15.



**Figure 2.15: Schematic representation of the electric field structure between parallel plate electrodes with a guard ring<sup>13</sup>**

### 2.3.5 Gravimetric Latex Drying Measurement

Drying experiments were conducted in an environmentally controlled chamber instrumented with a digital balance that continuously recorded the sample mass as shown in Figure 2.16. Prior to drying, latex epoxy resins were mixed with curing agents as described in Section 2.1.1. Resin samples were subsequently



withdrawn from a continuously stirred resin container with a syringe, which were then placed in the drying chamber to thermally equilibrate. Once equilibrated, each experiment was conducted by depositing approximately 5 ml of resin into 5.08 cm x 5.08 cm (2 inch x 2 inch) square silicone rubber molds suspended from the balance's load cell and beginning the mass measurement data acquisition. These molds were also equilibrated at the chamber temperature prior to beginning the experiment. Two series of experiments were conducted with temperature and humidity as variables: 32°C, 45°C and 63°C at a constant 15%RH; and 1.5% RH, 15 %RH, and 25 %RH at a constant 63°C. The temperature and humidity of the chamber were controlled to within  $\pm 2^\circ\text{C}$  and  $\pm 4\%$  RH, respectively. In most cases, two samples were measured for each resin formulation/drying condition, resulting in very good repeatability. Some of the higher DICY content/lower drying temperature experiments were conducted only once since the drying times were excessive and the accompanying resin film quality was obviously poor, as described in Section 3.2.5.1.

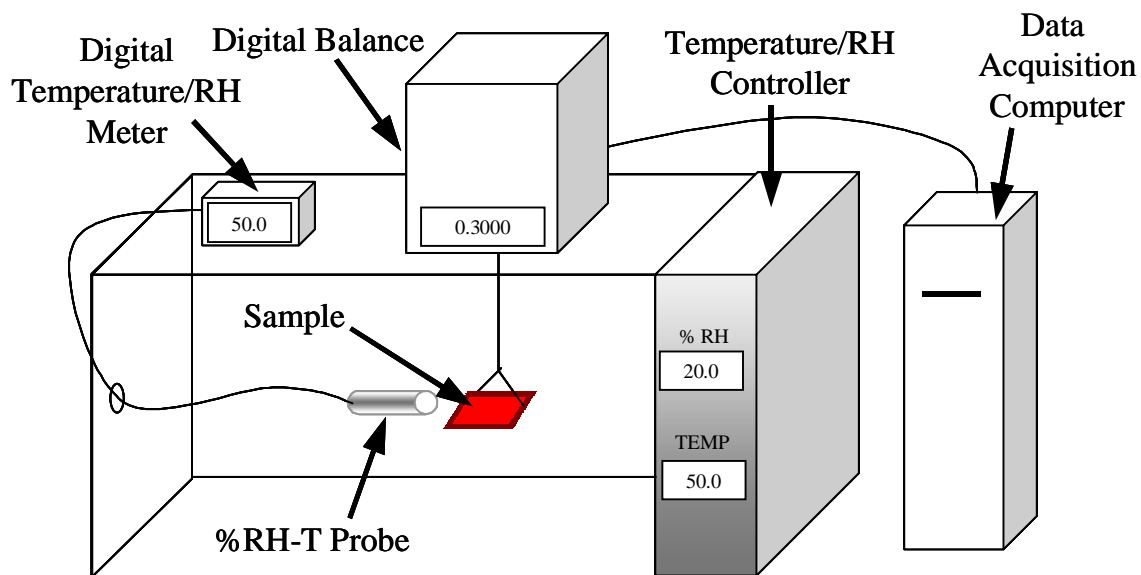


**Figure 2.16: Environmentally controlled drying chamber instrumented with a continuous weight monitoring system**

Waterborne epoxy impregnated glass cloth was dried in a similar manner. An 8.9 cm x 8.9 cm (3.5 inch x 3.5 inch) square of cloth was dip-impregnated through a resin bath, spread on a layer of teflon film, then placed on a glass plate. The weights of the dry glass cloth, the teflon film, and the glass plate were recorded prior to each experiment. The plate containing the impregnated sample was subsequently suspended from the balance and dried. Two samples were dried in each material system with good repeatability; the *maximum* standard deviation measured for drying rates for glass-supported latex samples represented 5.8 % of the mean.

## 2.3.6 Surface Analysis

### 2.3.6.1 X-ray Photoelectron Spectroscopy (XPS)

The elemental composition of a surface can be measured to depths of up to 100 Angstroms using XPS, also known as electron spectroscopy for chemical analysis (ESCA).<sup>14</sup> The XPS technique's high sensitivity at such small depths makes it ideal for characterization of failure interfaces in adhesion experiments. XPS can detect all elements, except for hydrogen and helium, by measuring the kinetic energies of electrons emitted from surface atoms during bombardment by X-ray radiation and computing their binding energies. This is an application of the photoelectric effect. The X-ray source is comprised of a filament that emits electrons that are subsequently accelerated through a high potential to strike a target anode. This anode emits X-ray photons having a characteristic energy,  $h\nu$ . The X-ray beam bombards the sample surface such that electrons from the sample's atoms are ejected and guided to a detector where they are counted based upon their kinetic energy KE. Given the known X-ray energy and the detected electron kinetic energy, the binding energy BE of the electrons can be computed by

$$\text{Equation 2.10} \quad BE = h\nu - KE - \phi_s$$

where  $\phi_s$  is the work function of the analyzer. The resulting spectrum is presented as the number of electrons counted by the detector as a function of binding energy.

The binding energies of electrons from different elements are distinct enough to allow accurate identification not only of that element, but its oxidation state as well. As the density of electrons in an atom decreases, the binding energy of the core electrons increases. Binding energy intensities can be used to quantify the relative amounts of various elements on a surface. Since different materials absorb X-rays with varying efficiency, sensitivity factors have been calculated to correct the observed intensities to specific species.<sup>15</sup> Electron escape depths, which are the limiting factor in analysis depth, vary depending on the type of the material surface; escape depths are 40 to 100 Å for polymers, 15 to 40 Å for oxides, and 5 to 20 Å for metals.<sup>15</sup>

The XPS analysis in this study was conducted using a Perkin Elmer PHI 5400 spectrometer with a Mg K $\alpha$  (1253.6 eV) X-ray source operated at 14 kV and 300W power. Vacuum chamber pressures at operation were at or below approximately  $5 \times 10^{-7}$  torr. For all samples a spot of 1 mm x 3 mm was analyzed at a 45° angle relative to the entrance of the electron analyzer. Spectra were corrected to an internal standard 284.6 eV corresponding to the binding energy of the carbon C 1s photopeak<sup>16</sup>; overall system calibration was to the gold 4f<sub>7/2</sub> photopeak at a binding energy of 83.7 eV<sup>17</sup>. A full width at half-maximum of  $1.7 \pm 0.1$  eV was used when curve fitting the C 1s peak. Two spots were analyzed on each sample. Binding energy peak location was accurate to 0.2 eV. All peak fits assumed Gaussian curves. Atomic concentrations were computed from peak areas using the equation<sup>14</sup>

Equation 2.11 
$$C_x = \frac{I_x / S_x}{\sum (I_i / S_i)}$$

where  $C_x$  is the atomic fraction of element x, I is the number of photoelectrons/second in a photopeak area, S is the area sensitivity factor. The denominator is a sum taken over all of the elements detected. An estimate of standard deviations associated with atomic concentration computation was 2.3 %<sup>14</sup>, except in the case of nitrogen detection in the presence of copper oxide surfaces where Cu LMM Auger emission interference increased the uncertainty. The detection limit for atomic concentration was 0.2%.

#### **2.3.6.2 Scanning Electron Microscopy (SEM)**

Micrographs of foil and adhesive fracture surfaces were obtained using an ISI-SX-40 scanning electron microscope operating at an acceleration voltage of 20kV. Samples were mounted on brass supports by double-sided tape, a conductive silver paint path was applied from the support face to a corner of each sample, and the ensemble was then sputtercoated with gold in an Edwards Sputter Coater S150B for two minutes. These steps were taken to provide good conduction to the brass mount, thereby minimizing sample charging.

#### **2.3.6.3 Diffuse Reflectance Infrared Fourier Transform Spectroscopy (DRIFTS)**

The chemistry of failure surfaces was analyzed by infrared spectroscopy using a variation of the DRIFTS technique developed for the analysis of powdered samples.<sup>18</sup> The instrument used to collect the IR spectra was a Nicolet 5DXB FT-IR spectrometer equipped with a DTGS KBr detector and external reflection accessories manufactured by Harrick Scientific Co. The sample chamber was continuously purged with dry nitrogen. A minimum of 5 minutes was allowed between sample insertion and the start of data collection to assure adequate purge. The mirror angle in the external reflection fixture was optimized iteratively to provide maximum signal, using a blank sample similar to those under investigation, prior to measurement of experimental samples. The optimum angle of incidence for glass-epoxy laminates was 68°. The spectral resolution was approximately 4 cm<sup>-1</sup>. A total of 500 scans was collected per spectrum. Background spectra were obtained by scanning the metal sample support after cleaning with acetone.

#### **2.3.6.4 Optical Microscopy**

Optical micrographs shown throughout this study were made in both the transmission and reflection modes using an Olympus BH-2 optical microscope fitted with an Olympus DP10 digital camera. Images were generally obtained using the lowest magnification objective lens (10x). The photograph stage lens had a magnification of 10x for a total magnification of 100x. All scales presented on optical micrographs were referenced to digital images of a 1mm stage micrometer, having a resolution of 0.01 mm, taken with the same lens combination used in analyzing the material sample. Polarizers were used in some images for filtering purposes.

### 2.3.6.5 Constituent Material Surface Characterization

SEM micrographs of the foils used in PCB laminate fabrication are shown, in the as-made condition, in Figure 2.17. Note the nodular surface morphology of the “brass” treated commercial foil in Figure 2.17 A and B. The etched and oxidized copper surface, produced by the process described previously, contains grooves from the abrasion step on the micron scale (Figure 2.17 D) with copper oxide crystals on the submicron scale (Figure 2.17 C).

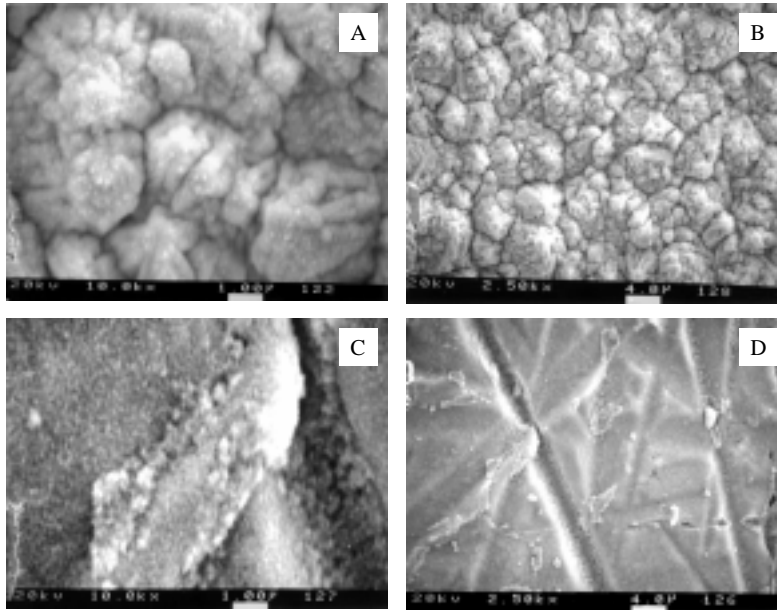


**Figure 2.17: SEM micrographs of as-made copper foil surfaces. (A) and (B): Zinc chromate “brass” treated, (C) and (D): abraded, etched, and sodium chlorite oxidized**

The surfaces of both types of treated copper foils, as well as the cured epoxy and glass material components of the PCB laminate, were characterized using XPS to determine their elemental composition. The atomic concentrations of these elements are listed in Table 2.1. The “brass” foil surface contains zinc and chromium from the zinc chromate treatment, but also contains a very low concentration of copper relative to the etched and oxidized copper foil. Atomic concentration data for the epoxy were obtained by fracturing neat resin bars and immediately examining the section plane by XPS. The compositions of the two epoxies are very similar; the presence of silicon is attributable to silica filler supplied with the DICY curing agent.

	%C	%O	%Cu	%Zn	%Cr	%S	%Cl	%Na	%Si	%Al	%Ca	%N
Brass surface	35.5	49.1	1.2	8.7	5.6	na	na	na	na	na	na	na
Etched-oxidized surface	27.4	43.9	27.0	na	na	0.2	0.3	1.2	na	na	na	na
Glass cloth	31.6	43.9	na	na	na	na	na	0.7	14.5	3.7	3.3	2.3
Bulk Epoxy Solvent	73.2	19.6	na	na	na	na	na	na	1.6	na	na	5.6
Bulk Epoxy Latex	77.8	19.1	na	na	na	na	na	na	0.9	na	na	2.2

**Table 2.1: XPS determined atomic concentrations of copper foil surfaces and laminate component materials [na: not analyzed; based on survey scan]**

## 2.4 References

- 
- <sup>1</sup> B. J. Love, PhD Dissertation, Southern Methodist University, 1990.
- <sup>2</sup> N. Shephard, Ph.D. Dissertation, VPI&SU, 1995, p.13-14.
- <sup>3</sup> G. Anderson, S. Bennett, and K. DeVries, Analysis and Testing of Adhesive Bonds, Academic Press, New York, 1977, p. 82-90.
- <sup>4</sup> A. N Gent and G. R. Hamed, Journal of Applied Polymer Science, Vol. 21, 1977, p. 2817.
- <sup>5</sup> ASTM Standard D2861-87, "Flexible Composites of Copper Foil with Dielectric Film or Treated Fabrics", 1993.
- <sup>6</sup> L. H. Sperling, Introduction to Physical Polymer Science, John Wiley & Sons, New York, 1992.
- <sup>7</sup> S. G. Hong and T. C. Wang, Journal of Applied Polymer Science, Vol. 52, 1994, p. 1339-1351.
- <sup>8</sup> H. Altschuler, in Handbook of Microwave Measurements, Third. ed., edited by M. Sucher and J. Fox, Polytechnic Press, New York, 1963, p. 495.
- <sup>9</sup> A. Metaxas and R. Meredith, Industrial Microwave Heating, Peter Peregrinus Ltd, London 1983 p. 39.
- <sup>10</sup> M. L. Jackson, M.S. Thesis, VPI&SU, 1993.
- <sup>11</sup> D. Kajfez and E. J. Hwan, IEEE Transactions on Microwave Theory and Techniques, MTT-32, 1984, p. 666.
- <sup>12</sup> TA Instruments DEA 2970 Dielectric Analyzer Operator's Manual, TA Instruments, New Castle, Delaware, 1997.
- <sup>13</sup> ATSM Standard D 1867-94, Standard Specification for Copper-Clad Thermosetting Laminates for Printed Wiring"
- <sup>14</sup> B. L. Holmes, M.S. Thesis, VPI&SU, 1994, p.41.

---

<sup>15</sup> W. M. Riggs and M. J. Parker, "Surface Analysis by X-Ray Photoelectron Spectroscopy" in *Methods and Phenomena 1: Methods of Surface Analysis*, Ed. A. W. Czanderna, Elsevier Science Publishers, New York, 1989, p. 103.

<sup>16</sup> C. D. Wagner, W. M. Riggs, L. E. Davis, J. F. Moulder, *Handbook of X-Ray Photoelectron Spectroscopy*, Ed. G. E. Muilenberg, Perkin-Elmer Corporation, Eden Prairie, MN 1979.

<sup>17</sup> J. C. Fuggle and N. Martenssoon, *Journal of Electron Spectroscopic Related Phenomena*, Vol. 21, 1980, p. 275.

<sup>18</sup> S. R. Culler, "Diffuse Reflectance Infrared Spectroscopy: Sampling Techniques for Qualitative/Quantitative Analysis of Solids", in *Practical Sampling Techniques for Infrared Analysis*, Ed. P. B. Coleman CRC Press, Boca Raton, FL, 1993, p.93.